Environmental Science & Technology

pubs.acs.org/est

Article

Trends of Diverse POPs in Air and Water Across the Western Atlantic Ocean: Strong Gradients in the Ocean but Not in the Air

Rainer Lohmann,* Erin Markham, Jana Klanova, Petr Kukucka, Petra Pribylova, Xiangyi Gong, Robert Pockalny, Tatyana Yanishevsky, Charlotte C. Wagner, and Elsie M. Sunderland

Cite This: https://dx.doi.org/10.1021/acs.est.0c04611

Read Online

ACCESS | Metrics & More | Article Recommendations | Supporting Information

ABSTRACT: Oceans have remained the least well-researched reservoirs of persistent organic pollutants (POPs) globally, due to their vast scale, difficulty of access, and challenging (trace) analysis. Little data on POPs exists along South America and the effect of different currents and river plumes on aqueous concentrations. Research cruise KN210-04 (*R/V Knorr*) offered a unique opportunity to determine POP gradients in air, water, and their air−water exchange along South America, covering both hemispheres. Compounds of interest included polychlorinated biphenyls (PCBs), organochlorine pesticides (OCPs), polybrominated diphenylethers (PBDEs), and polycyclic aromatic hydrocarbons (PAHs). Remote tropical Atlantic Ocean atmospheric concentrations varied little between both hemispheres; for HCB, BDEs 47 and 99, they were ∼5 pg/m^3, PCBs were ∼1 pg/m^3, α-HCH was ∼0.2 pg/m^3, and phenanthrene and other PAHs were in the low 100s pg/m^3. Aqueous concentrations were dominated by PCB 52 (mean 4.1 pg/L), HCB (1.6 pg/L), and β-HCH (1.9 pg/L), with other compounds <1 pg/L. Target PCBs tended to undergo net volatilization from the surface ocean, while gradients indicated net deposition for *a*-HCH. In contrast to atmospheric concentrations, which were basically unchanged between hemispheres, we detected strong gradients in aqueous POPs, with mostly nondetects in the tropical western South Atlantic. These results highlight the importance of currents and loss processes on ocean scales for the distribution of POPs.

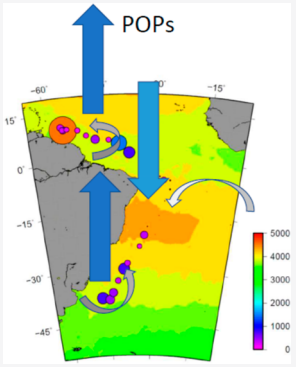

INTRODUCTION

Persistent organic pollutants have been detected all across the globe[1] including the atmosphere,[2] terrestrial environments,[3] food-webs,[4] the poles,[5,6] the ocean sediment,[7,8] and water column.[9] Many studies on the global distribution of POPs were initiated by Kevin C. Jones, his research group, and collaborators to whom this article and Special Issue is dedicated.

Pioneering work by Iwata et al. (1993) started the first global assessment of POPs in the Oceans[10] though it is unclear if any of the results were affected by ship-based contamination.[11] Since their landmark publication, there has been only one other study addressing POPs in oceans on a global scale, the Malaspina cruise (2010−2011).[12−14] For several ocean basins, there has been repeated coverage of air−water exchange and spatial gradients of POPs: initially, with a focus on North Atlantic/Arctic Ocean and eastern part of the Atlantic Ocean where ships of opportunity (often polar research vessels) transited.[15−18] More lately, some more coverage of POPs in the Pacific Ocean has been published with increasing use of the Chinese Snow Dragon.[19,20] Little to no work remains published on POPs in the Indian Ocean, Southern Ocean,[21,22] and western part of The Atlantic Ocean, along South America.

While atmospheric studies have long shown that, far removed from point sources, the atmosphere is fairly well mixed and has general low POP concentrations, the knowledge of oceans is less well developed. Ideas of well mixed ocean basins (as used in simple models) do not hold true. While there are studies to show minor gradients in concentrations of extremely persistent compounds, e.g., perfluorooctanoic acid (PFOA) and perfluorooctanesulfonic acid (PFOS) between the North and South Atlantic, there is also evidence that currents and river discharges actually maintain strong gradients in POPs concentrations far away from shore.[23,24]

So ironically, while oceanographers would say there is only 1 ocean, in terms of POPs, one could argue that there are 2 atmospheric cells (northern hemisphere, NH, and southern hemisphere, SH) but, indeed, several distinct ocean basins.

Research cruise KN210-04 of the *R/V Knorr* in March−May 2013 from Uruguay to Barbados offered a unique opportunity to determine POPs' gradients in air, water, and their air−water exchange (Figure 1). The cruise track covered a fairly large north−south gradient along the South-American coast and

Special Issue: POPs on the Global Scale: Sources, Distribution, Processes, and Lessons Learned for Chemicals Management

Received: July 12, 2020
Revised: October 17, 2020
Accepted: October 27, 2020

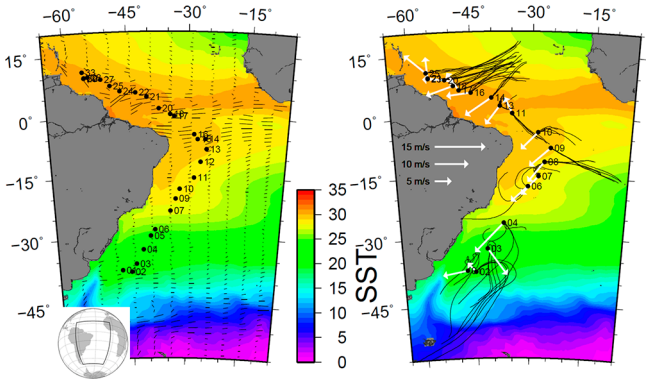

Figure 1. Sample locations for water and air samples taken on the *RV Knorr* KN210-04 from Montevideo, Uruguay to Bridgetown, Barbados, March−May 2013. (a) Typical surface current velocities. (b) Direction and magnitude of true wind measured on the ship (white arrows) and NOAA's 5-day backtrajectory HY-SPLIT analysis (black lines).[31,32] Maps produced in Generic Mapping Tools (5);[57] Sea Surface Temperature 10-year average (2008−2017) from data obtained NASA SST Aqua MODIS Web site;[58] Ocean Currents.

along Brazil into the Caribbean, so far unexplored in terms of POPs concentrations and fluxes, far away from shore. In particular, the cruise covered a region that is influenced by 2 major river plumes: the Rio de la Plata in the southern tropical Atlantic Ocean, and the Orinoco and Amazon River plumes north of the equator. In-between those plumes, the South Equatorial Current brings water masses from along Africa (Benguela Current) toward Brazil, where the water masses split into the North Brazil and Brazil Currents. Previous cruises established only small gradients in dissolved POPs along Africa, but it is unknown how ocean transport and atmospheric deposition might affect POPs on the South American side of the tropical Atlantic Ocean.

In summary, we analyzed samples collected across the western Atlantic to (i) determine whether there were significant POPs gradients in air or water between NH and SH in this region, (ii) assess whether the Atlantic Ocean was a net sink or secondary source of gas-phase PCBs, OCPs, PBDEs, and PAHs, (iii) identify whether ocean current and river plumes would affect the presence and air−water gradients of selected POPs, and (iv) compare our measurement with results obtained from a coupled global circulation model for PCBs.

METHODS

Sampling. *High Volume Water Sampling.* Sampling was conducted from March 25−May 9, 2013 between Uruguay and Barbados. Active air and water sampling procedures were as described elsewhere.[23] A total of 33 water samples were collected in the ship's laboratory from the ship's seawater pipe using a sampling train, equipped with a precombusted glass fiber filter (GFF, 142 mm Whatman GF/F, 0.7 μm retention) and 3 polyurethane foam (PUF) plugs in series (see Table S1). The average flow rate was generally around 0.8−1 L/min with an average volume of 736 L (see SI).

High Volume Air Samples. For air, a high volume Tisch Environmental Air Sampler was employed to pass air first through a quartz fiber filter (QFF, Whatman GF/A, 1.6Q-MA, 25 cm × 30 cm, 2.2 μm retention), and then 2 pre-extracted PUF plugs. The active air sampler was setup at the front of the monkey's level (above the bridge), facing the wind. Air samples were only started when the wind was forward of the beam and wind direction was monitored throughout transits. A total of 25 air samples (including 6 blanks) were collected (see Table S2). The sampler was fairly consistent, pumping air at an average rate of 38 m^3 of air per hour. The target volume of air was 750 m^3; however, due to time constraints of transit and issues of wind shifts and ship maneuvers, some samples had a smaller volume.

PE Sheet Samplers. Potential background laboratory contamination was measured using polyethylene (PE) passive samplers. PE sheets were placed in various locations on the ship for the duration of the cruise (ca. 6 weeks) to be extracted and analyzed for potential background contamination (see Table S7).

Sample Analysis. *High Volume Samples (PUFs, GFFs).* Analytical standards for PBDEs (calibration sets, natives and mass labeled) were purchased from Wellington Laboratories (Canada). Standards for PAHs, indicator PCBs, and OCPs were purchased from LGC (UK). PUFs and GFFs were combined and extracted using automated warm Soxhlet extraction (40 min warm Soxhlet followed by 20 min of solvent rinsing) with dichloromethane (DCM) in a B-811 extraction unit (Büchi, Switzerland). For several samples, GFFs were analyzed individually, with no compounds detected above MDLs. Prior to extraction, the samples were spiked with ^{13}C BDEs (28, 47, 100, 99, 154, 153, 183, and 209) for PBDE analysis, PCB 30 and 185 for PCB and OCP analysis, and deuterated PAHs (d_8-naphthalene, d_{10}-phenathrene, d_{12}-perylene) for PAH analysis. The concentrated extracts were split into 2 portions: one part of the extract was used for PAHs analysis; another part of the extract was analyzed for PBDEs, indicator PCBs, and OCPs.

PE Sheet Samplers. Blanks and exposed PE sheets were rinsed with Milli-Q water (Millipore, Billerica, MA), dried with a disposable tissue, and soaked for 24 h in 200 mL *n*-hexane followed by 24 h in 200 mL DCM. The two solvents were then pooled and concentrated under nitrogen in a TurboVap II concentrator, and the extract was split into 2 portions and processed using the same procedure as the high volume samples.

PAH Analysis. The first portion of extract was fractionated on a silica column (5 g of silica 0.063−0.200 mm, activated at 150 °C for 12 h). The first fraction (10 mL *n*-hexane) containing aliphatic hydrocarbons was discarded. The second fraction (20 mL DCM) containing PAHs was collected and then reduced by stream of nitrogen in a TurboVap II (Caliper LifeSciences, USA) concentrator unit and transferred into a vial. Terphenyl was added as syringe standard for a 100 μL final volume. GC-MS analysis was performed on 7890A GC (Agilent, USA) equipped with a 60 m × 0.25 mm × 0.25 μm DB5-MSUI column (Agilent, J&W, USA) coupled to 7000B MS (Agilent, USA) (for more details, see the SI).

PBDE, Indicator PCB and OCP analysis. The second portion of extract was cleaned-up on a H_2SO_4 modified (44% w/w) silica column; analytes were eluted with a 30 mL DCM/*n*-hexane mixture (1:1). The eluate was concentrated using a stream of nitrogen in a TurboVap II concentrator unit and transferred into an insert in a vial. The syringe standards (^{13}C BDEs 77 and 138 and native PCB 121) were added to all samples for a 100 μL final volume.

HRGC/HRMS instrumental analysis (for PBDEs) was performed on 7890A GC (Agilent, USA) equipped with a 15 m × 0.25 mm × 0.10 μm RTX-1614 column (Restek, USA)

https://dx.doi.org/10.1021/acs.est.0c04611
Environ. Sci. Technol. XXXX, XXX, XXX−XXX

coupled to AutoSpec Premier MS (Waters, Micromass, UK) in EI+ mode (for more details, see the SI).

GC-MS/MS was used for indicator PCBs and OCPs analysis. 7890A GC (Agilent, USA) equipped with a 60 m × 0.25 mm × 0.25 μm HT8 column (SGE, USA) coupled to 7000B MS (Agilent, USA) operated in EI+ MRM was used (for more details, see the SI).

Quality Assurance, Quality Control, Data Treatment. Recoveries of *d*-PAHs were on average 40% (d-naphthalene), 76% (*d*-phenanthrene), and 65% (*d*-perylene) and ranged from 40−91% for the ^{13}C-PBDEs. Recoveries of a reference material (spiked PUFs and GFFs) ranged from 45 to 64% (PCB 30) and 72−98% (PCB 185). Results were not recovery corrected, except for PBDEs.

Four field blanks each were analyzed for water and air PUFs and GFFs, 5 for PEs. Field blanks were mounted as real samples, shortly turned on, and recovered. The final concentrations were blank corrected. The method detection limit (MDL) was calculated as 3 standard deviations of blank concentrations (see Tables S4−S6). Concentrations <MDL were substituted with 1/2 MDL in cases where ≥50% of data were > MDL, even though a 70% data coverage is preferred.[25]

Physicochemical Properties. Octanol−water (K_{ow}) and air−water partitioning (K_{aw}) ratios, and aqueous solubility at saturation of the subcooled liquid (C_{iw}^{sat} (L) were taken from internally consistent data compilation whenever possible (see Table S3).[26,27] For all compounds, average values were taken for enthalpies of PE-water (25 kJ mol^{-1}) and PE-air exchange (80 kJ mol^{-1}), close to calculated values of internal octanol−water and octanol-air exchange.[26,27] The Setschnow constant was taken as 0.35, as reported elsewhere.[28] K_{aw} and dissolved concentrations were not corrected for the influence of dissolved organic carbon (DOC), as DOC concentrations in the open Ocean[29] are in general too low to sorb more than a few% of the most hydrophobic PCBs assuming general DOC affinities to POPs.[30]

Fraction on Particles. For 2 samples each (water and air), GFFs (particle-bound fraction) were extracted separately from PUFs (dissolved or gas-phase fraction), and the particle-bound fraction was determined as (see Tables S14 and S15)

$$\%particle - bound = \frac{C_{particulate}}{C_{gas}(C_{diss}) + C_{particulate}} \quad (1)$$

where C_{gas} (C_{diss}) is the gas-phase (dissolved phase concentration (pg/L), and $C_{particulate}$ is the particle-bound concentration (pg/L).

Meteorological and Sea Surface Auxiliary Measurements. From the ship's routine measurements, we averaged values of latitude, longitude, surface water temperature (T_{water}), salinity, and fluorescence of the flow-through seawater; air temperature (T_{air}), relative humidity (RH), relative and absolute wind speeds, and directions were recorded every minute for each sampling period (see Tables S1, S2). Back-trajectories were back-calculated for 5 days with four 6 h steps for each average sample location at 500 m above sea level using HYSPLIT (see Figure 1).[31,32]

Air−Water Exchange. Fugacity gradients across the air−water interface were calculated, f_{aw}, such that values >0 indicated net volatilization, 0 indicated equilibrium, and <0 indicated net deposition:

$$f_{aw} = 1 - \frac{C_{gas}}{C_{diss} \times K_{aw}(T, salinity) \times 10^3} \quad (2)$$

where C_{gas} is the gas-phase concentration (pg/m^3), C_{diss} is the dissolved phase concentration (pg/L), and $K_{aw}(T, \text{salinity})$ is the dimensionless air−water partitioning coefficient corrected for temperature (T) and salinity.

Ocean Model. Modeled PCB concentrations in the global oceans and air-sea exchange fluxes were based on a 3-D ocean simulation developed by Wagner et al., (2018).[33] The PCB simulation is embedded in the Massachusetts Institute of Technology general circulation model (MITgcm) and has a horizontal resolution of 1° × 1° degrees in most regions and 23 vertical levels. It is forced by atmospheric PCB concentrations and deposition fluxes from a global atmospheric PCB simulation embedded in GEOS-Chem atmospheric chemical transport model and simulates the oceanic fate of the 1930−2015 global release inventory developed by Breivik et al.[34−36]

Cruise Track. Samples were exclusively taken outside the countries 200 (nautical mile) exclusive economic zones (EEZs). Water samples up to 30°S (Nos 1−4) showed some influence of the Rio de la Plata plume,[37] as indicated by lower salinity; samples 30−5°S (5−12) were influenced by the Brazil Current, which moves water from the South Equatorial Current (SEC) across the tropics; the SEC directly affected samples taken below the equator (13−17), while samples taken between the equator and 5°N (20−24) were influenced by the Brazil Current, which is an extension of the SEC along the continent; the last few samples were affected by the Amazon River plume, as was also indicated by decreased salinity for samples 28−33 (Figure 1a).

Atmospherically, the air sampled in-between 38°S and 30°S (Air 1−4) originated from the Southern Ocean/South Atlantic Ocean. Samples between 30°S and the equator (Air 6−11) originated from the Central southern Atlantic Ocean. Samples taken just north of the equator (Air 13) indicated the influence of the Inter Tropical Convergence Zone (ITCZ), while air samples taken from 4°N and north all originated from the northern hemisphere: samples 13−25 originated from the southern part of the North Atlantic Ocean (Figure 1b).

Indoor PE Sheets. For the in-ship exposed passive samplers, PE-air (K_{PEa}) equilibrium partitioning constants were taken at 298 K and converted to gas-phase concentrations assuming equilibrium had been reached. PCB 28 dominated indoor air, at 2800−8700 pg/m^3, followed by PCB 52 (440−1200 pg/m^3), HCB/PeCB (100−300 pg/m^3 each), and PCB 101 (60−160 pg/m^3). The other analytes were at or below 10 pg/m^3 or below detection limits (see Table S7). For PAHs, concentrations of ∼1 ng/m^3 were observed for pyrene and fluoranthene, and >10 ng/m^3 for phenanthrene (Table S7). Importantly, the ratios of fluoranthene/pyrene and retene/pyrene were distinctly different between in-ship and marine boundary layer samples collected on-board (Figure S1). In summary, while there is potential for contamination of samples with handling inside the R/V Knorr, the PAH profiles imply little to no evidence of contamination.

RESULTS AND DISCUSSION

Air Concentrations of PCBs and OCPs. HCB and α-HCH were detected in all atmospheric samples. All other target OCPs were only detected above MDL in two (γ-HCH, PeCB) or fewer samples (see Table S8). Atmospheric concentrations were dominated by HCB (mean 8.8 pg/m^3;

https://dx.doi.org/10.1021/acs.est.0c04611
Environ. Sci. Technol. XXXX, XXX, XXX−XXX

Table 1. Summary of Air and Water Concentrations of the Most Abundant PCBs/OCPs, PBDEs, and PAHs[a]

	AIR (pg/m3)								WATER (pg/L)						
PCBs/OCPs	min	max	mean	median	count	MDL	% det.		min	max	mean	median	count	MDL	% det.
PCB 28	<MDL	15	<MDL	<MDL	8	8.1	42%	PCB 28	<MDL	55	<MDL	<MDL	3	6.8	11%
PCB 52	<MDL	9.2	<MDL	<MDL	8	4.3	42%	PCB 52	<MDL	24	<MDL	<MDL	4	3.1	14%
PCB 101	<MDL	1.7	<MDL	<MDL	4	1.3	21%	PCB 101	0.1	3.4	0.7	0.5	17	0.3	100%
PCB 118	<MDL	0.6	<MDL	<MDL	8	0.3	42%	PCB 118	0.0	2.5	0.5	0.3	18	0.1	100%
PCB 153	<MDL	0.6	<MDL	<MDL	3	0.5	16%	PCB 153	0.0	1.2	0.2	0.1	14	0.1	100%
PCB 138	<MDL	0.4	<MDL	<MDL	7	0.2	37%	PCB 138	0.0	0.9	0.2	0.1	15	0.0	100%
PCB 180	<MDL	0.2	<MDL	<MDL	4	0.1	21%	PCB 180	<MDL	0.4	<MDL	<MDL	7	0.1	25%
HCB	4.9	15	8.8	7.7	19	0.6	100%	HCB	<MDL	12	<MDL	<MDL	7	0.7	25%
a-HCH	0.2	0.6	0.3	0.3	19	0.0	100%	a-HCH	<MDL	0.6	0.3	0.2	13	0.1	46%
b-HCH	<MDL	<MDL	<MDL	<MDL	0	1.4	0%	b-HCH	0.3	3.5	1.5	1.6	19	0.7	100%
g-HCH	<MDL	1.5	<MDL	<MDL	2	0.9	11%	g-HCH	<MDL	1.2	<MDL	<MDL	7	0.5	25%
PBDEs															
BDE 28	0.3	1.2	0.7	0.7	14	0.1	100%	BDE 28	<MDL	0.2	<MDL	<MDL	8	0.0	35%
BDE 47	2.4	9.4	5.8	5.3	14	1.8	100%	BDE 47	<MDL	7.0	<MDL	<MDL	8	1.2	35%
BDE 66	0.0	0.5	0.2	0.2	12	0.1	100%	BDE 66	<MDL	3.1	<MDL	<MDL	2	0.0	9%
BDE 100	0.3	1.3	0.6	0.5	14	0.3	100%	BDE 100	<MDL	1.8	<MDL	<MDL	7	0.2	30%
BDE 99	0.6	5.7	2.2	2.0	8	2.1	100%	BDE 99	<MDL	3.6	<MDL	<MDL	1	1.4	4%
BDE 154	0.0	0.4	0.1	0.1	10	0.1	100%	BDE 154	<MDL	0.2	<MDL	<MDL	1	0.1	4%
BDE 153	<MDL	0.4	<MDL	<MDL	4	0.1	29%	BDE 153	<MDL	<MDL	<MDL	<MDL	0	0.1	0%
BDE 183	0.0	0.2	0.1	0.0	7	0.1	100%	BDE 183	<MDL	2.4	<MDL	<MDL	10	0.0	43%
BDE 209	<MDL	310	<MDL	<MDL	6	14	43%	BDE 209	<MDL	34	<MDL	<MDL	2	9.0	9%
PAHs															
Phenantrene	82	2400	760	560	17	200	100%	Phenantrene	<MDL	4000	<MDL	<MDL	1	1800	4%
Antracene	8	84	35	29	13	18	100%	Antracene	<MDL	<MDL	<MDL	<MDL	0	98	0%
Fluoranthene	40	530	140	73	9	96	100%	Fluoranthene	<MDL	1300	<MDL	<MDL	1	540	4%
Pyrene	67	1200	250	120	9	160	100%	Pyrene	<MDL	1900	<MDL	<MDL	1	760	4%
Retene	12	900	100	50	14	29	100%	Retene	<MDL	<MDL	<MDL	<MDL	0	260	0%
Benzo(ghi)flA	0	380	30	7	17	4	100%	$_{l}A)_{r}l_{h}i(g_{o}$(zneB	<MDL	<MDL	<MDL	<MDL	0	180	0%

[a]MDL derived as 3 st.dev of mean blank values divided by average sampling volumes (664 m^3 air; 736 L water). N = 19 (air), 28 (water), except for PBDEs where n = 14 (air) and 23 (water).

https://dx.doi.org/10.1021/acs.est.0c04611
Environ. Sci. Technol. XXXX, XXX, XXX−XXX

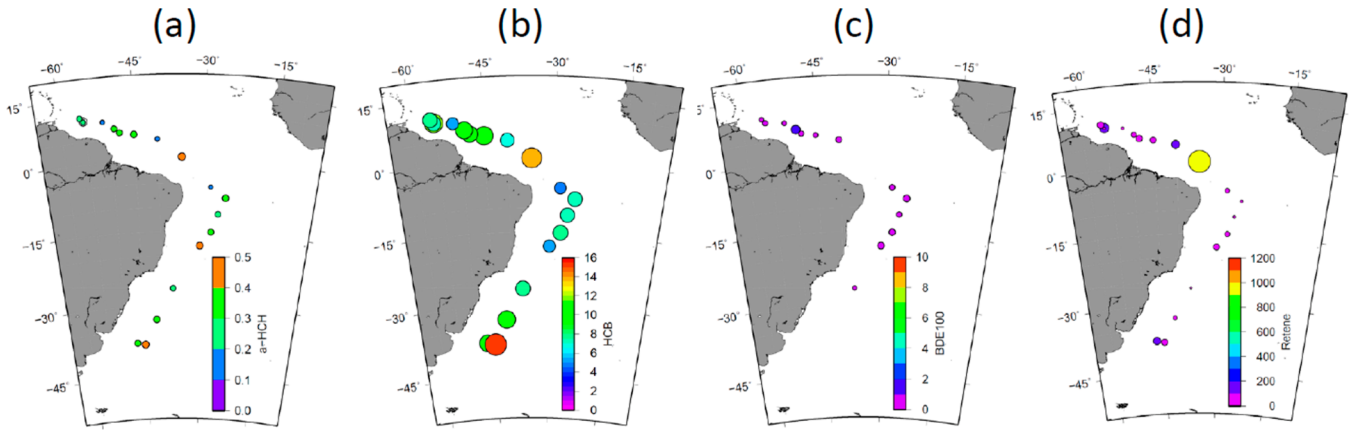

Figure 2. Atmospheric concentrations of (a) α-HCH, (b) HCB, (c) BDE 100, and (d) retene (pg m^{-3}) as a function of latitude.

median 7.7 pg/m^3); a-HCH was present at an average of <1 pg/m^3 (mean 0.32; median 0.33 pg/m^3), (see Table 1).

In the air, PCB congeners 28, 52, and 118 were detected in about half the total samples; other congeners displayed fewer concentrations above MDLs. There were minor, nonsignificant differences between concentrations of individual PCBs and OCPs in the gas-phase of the NH and SH (Figure 2). PCBs and OCPs were only detected on PUFs, implying that they were predominantly in the gas-phase (see Table S14).

Similar gas-phase concentrations of PCBs and HCB were reported by Lohmann et al.[23] for the tropical Atlantic Ocean and Zhang et al.[38] for PCBs in the North Atlantic Ocean near Iceland. Concentrations on the order of 10 pg/m^3 were reported for PCBs, DDTs, and HCHs for samples collected in coastal/offshore South America, and HCB at a few pg/m^3 at those same locations.[39]

Air Concentrations of PBDEs. Most targeted PBDEs were regularly detected in atmospheric samples. BDEs 28, 47, and 100 were detected in all samples analyzed, while BDEs 66 and 154 were detected in most samples and other congeners less frequently (Table S10). If detected above MDL (6 out of 14), BDE 209 was present at the greatest concentrations (up to 310 pg/m^3). Of all other BDE congeners, only BDEs 47 (mean 5.8 pg/m^3) and 99 (mean 2.2 pg/m^3) were present at concentrations >1 pg/m^3. Unexpectedly, there were no significant differences between both hemispheres (Figure 2).

When measured, BDE 209 also generally dominated in previous studies;[40,41] next highest concentrations were reported for BDEs 47 and BDE 99. For samples taken in the Atlantic Ocean marine boundary layer, the range of mean BDE 47 concentrations was 0.3−3 pg/m^3, and 0.2−0.9 pg/m^3 for BDE 99.[40] Lohmann et al. reported similar concentrations for various atmospheric PBDEs for an East-to-west transect, including the dominance of BDE 209, BDEs 47 and 99 > 1 pg/m^3, and the detection of other PBDE congeners.[41]

Air Concentrations of PAHs. A wide range of PAHs was detected in the atmosphere: Greatest concentrations were recorded for phenanthrene (average 760 pg/m^3, median 560 pg/m^3, detected in 89% of samples), followed by pyrene (250 pg/m^3, median 120 pg/m^3, 47%), fluoranthene (140 pg/m^3, median 73 pg/m^3, 47%), and retene (100 pg/m^3, median 50 pg/m^3, 74%). Benzo(ghi)perylene and anthracene were also detected in most samples at average concentrations below 50 pg/m^3. Other PAHs were detected irregularly at tens of pg/m^3 or below. In general, lower concentrations were reported for higher weight-molecular PAHs (see Table S12). Typically, over 95% of PAHs were detected in the gas-phase (see Table S14).

The potential source identification based on molecular ratios of PAHs derived from long-range is difficult, as even small differences in (direct and indirect) photolysis reaction rates and washout ratios of PAHs affect these ratios (for more details see the SI). The regular presence of retene in atmospheric samples likely indicates biomass burning as a dominant emission source.[42]

Ma et al. (2013) reported similar concentrations of atmospheric PAHs in the Northern Pacific Ocean boundary layer[43] and a preponderance of most PAHs in the gas-phase, similar to results by Lohmann et al. (2013) for the tropical Atlantic Ocean.[44] Somewhat greater concentrations of PAHs were reported by Gonzalez-Gaya et al. (2016) for atmospheric PAHs across the global oceans.[45]

Overall, a comparison to prior published work implies that the atmospheric concentrations summarized here for the western Atlantic Ocean represent typical values which were not strongly impacted by ship-based sampling artifacts or contamination.[11]

Atmospheric Pollutant Gradients Across the Western Tropical Atlantic Ocean. Trends in atmospheric concentrations were roughly similar for PCBs/OCPs, PBDEs, and PAHs. Elevated atmospheric concentrations were displayed south of 30°S, closest to the Rio de la Plata estuary (Figure 2), though winds were mostly coming from the southern part of the South Atlantic Ocean (Figure 1b). There were only minor gradients in atmospheric concentrations between 30°S and the equator; e.g., α-HCH varied from 0.16 to 0.41 pg/m^3, while the more persistent HCB fluctuated from 4.9 to 7.7 pg/m^3. Phenanthrene varied also by about 2-fold, from 500−1200 pg/m^3, and similarly small variations were observed for PBDEs 47 and 99 and the PCBs, though several were at times below MDLs. Overall, this suggests that we repeatedly sampled the remote southern hemispheric Atlantic Ocean marine boundary layer.

Once the ship crossed the ITCZ, just north of the equator, there was surprisingly little change in atmospheric concentrations, though the marine boundary layer air we sampled now originated from the remote tropical northern hemispheric Atlantic Ocean. By and large, then, we can summarize that remote tropical Atlantic Ocean concentrations of HCB, BDEs 47 and 99 are ~5 pg/m^3 (±2.5 pg/m^3), PCBs around single pg/m^3, α-HCH below ~1 pg/m^3, and phenanthrene and other PAHs in the low 100s pg/m^3.

https://dx.doi.org/10.1021/acs.est.0c04611
Environ. Sci. Technol. XXXX, XXX, XXX−XXX

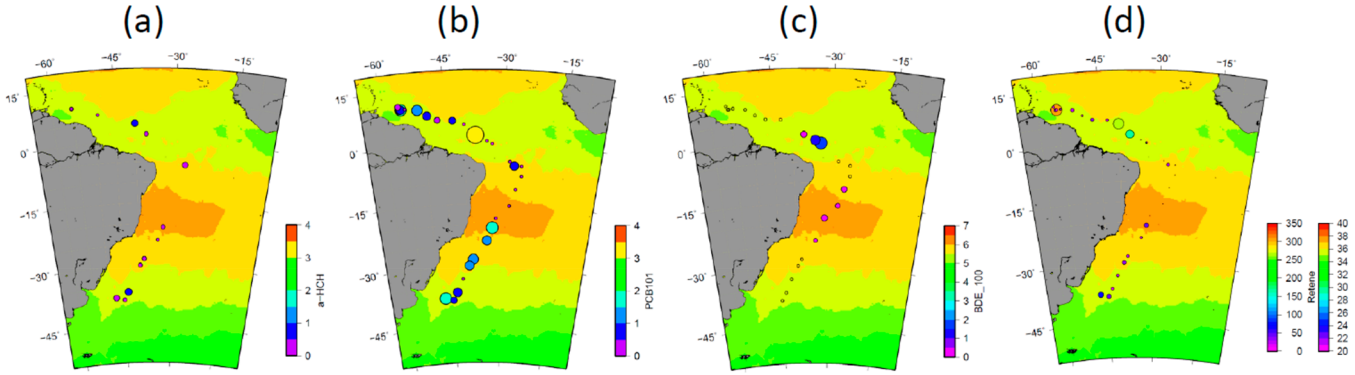

Figure 3. Aqueous concentrations of (a) α-HCH, (b) PCB 101, (c) BDE 100 and (d) retene (pg L^{-1}) as a function of latitude.

While our sampling locations represent background marine boundary layers in both hemispheres and are strongly affected by the movement of the ITCZ, these results could indicate a broader shift toward a redistribution of PCBs and OCPs after their phase-out almost 50 years ago, leading toward homogeneous atmospheric concentrations in both hemispheres.

However, several POPs displayed elevated atmospheric concentrations just north of the equator (e.g., PCBs 28 and 52 and several PAHs), which agrees with previously reported results for dissolved and gaseous mercury and is consistent with the pattern of deep convection and deposition around the ITCZ with elevated precipitation depositing compounds back to the surface oceans.[46] Given the seasonal movement of the ITCZ, there could be a strong coupling of precipitation of gas-phase POPs causing a spike in aqueous concentrations (see below; Figure 3), which in turn would cause revolatization to the atmosphere. We also observed increased aqueous concentrations just north of the equator but cannot prove that the two are causally linked.

Water Concentrations of PCBs and OCPs. The detection of PCBs and OCPs in water samples was bimodal, with general detection of compounds between 2 and 11°N (n = 11 samples) and 20 to 38°S (n = 8). Between those two regions, most compounds were not detected above MDL (n = 9), with the exception of a single sample taken at 6°S. PCBs 101, 118, 138, and 153 were detected in over half of all samples, as was β-HCH. Aqueous concentrations were dominated by PCB 101 (mean 0.72 pg/L; median 0.53 pg/L), and β-HCH (mean 1.5 pg/L; median 1.6 pg/L), with other compounds generally below 1 pg/L (see Table S9). PCBs and OCPs were only detected on PUFs, but not on GFFs, implying that they were predominantly in the dissolved-phase (see Table S15).

Concentrations of most PCB congeners and OCPs were basically the same in both hemispheres, with a couple of unusually high concentrations detected just north of the equator. Spikes in concentrations of POPs near the equator agree with previously reported results for dissolved and gaseous mercury and are consistent with the patterns of deep convection and deposition around the ITCZ with elevated precipitation returning compounds back to the surface oceans.[46] As noted above, we observed several POPs in the gas phase just north of the equator.

During a trip traversing the tropical Atlantic Ocean, Lohmann et al. (2012) routinely detected PCBs 52, 101, and 118 in the dissolved phase, mostly <1 pg/L. Greater concentrations were reported for hexachlorobenzene (HCB), ranging from 0.1−3 pg/L; HCHs were only detected close to the U.S. Eastern Coast, at <46 pg/L (α- HCH) and 8 pg/L (β-HCH). Results from passive sampling indicated the presence of DDTs below 1 pg/L across the tropical Atlantic Ocean.[23] Similar concentrations were also reported for PCBs during the North Atlantic Bloom experiments in 2008.[38] Concentrations of PCBs and OCPs that were slightly more elevated were reported by Lammel et al.[47] for the tropical Atlantic Ocean.

Water Concentrations of PBDEs. When detected, BDE 209 dominated overall concentrations at >10 pg/L. BDE 183 was most regularly detected (43%) at 0.51 pg/L, followed by BDEs 47 (35%, at 3.0 pg/L) and BDE 28 (35% at 0.09 pg/L). There were no significant differences between both hemispheres (see Table S11).

Dissolved concentrations of PBDEs were slightly higher than those reported earlier for PBDEs in different ocean basins, probably due to a combination of time trends of PDBEs leaching into remote environments[48] and analytical approaches by different laboratories in measuring PBDEs. Lohmann et al.[41] reported concentrations of ∼0.5 pg/L for BDE 47 and around 0.1 pg L−1 for BDEs 28, 99, and 100 on transect across the tropical Atlantic Ocean. These concentrations were based on passive sampling, which would only take up freely dissolved PBDEs. Xie et al. (2011) measured water samples for PBDEs in the Eastern Atlantic Ocean on a R/V Polarstern cruise in 2008 and reported around 0.1 pg L−1 for BDEs 47 and 99 and a factor of 10 lower for other PBDEs.[22] More recently, Wu et al.[49] published concentrations of PBDEs in the surface waters of the East China Sea and Northwest Pacific Ocean. BDE 209 displayed the greatest concentrations (2.7 pg/L), followed by BDE 47 (0.3 pg/L) and BDE 99 (0.13 pg/L).

Water Concentrations of PAHs. While PAHs were rarely detected above MDLs in the water (see Table S13), we can report that the same trends could be seen as those for the other POPs above, namely, a clear difference in concentrations as a function of ocean region. Over 95% of PAHs were detected in the dissolved phase (on PUFs) rather than being particle-bound (on GFFs) (see Table S15).

Dominant PAHs were phenanthrene, pyrene, and fluoranthene, similar to what we observed in the atmosphere. Key PAHs (phenanthrene, pyrene, fluoranthene) were present at 100s pg/L between 20 to 38°S (n = 8) and even greater amounts between 2 and 11°N (n = 11 samples). Between 20°S and 1°N (n = 9), mean (and median) concentrations were much lower: phenanthrene at 31 (11) pg/L, pyrene at 19 (2)

https://dx.doi.org/10.1021/acs.est.0c04611
Environ. Sci. Technol. XXXX, XXX, XXX−XXX

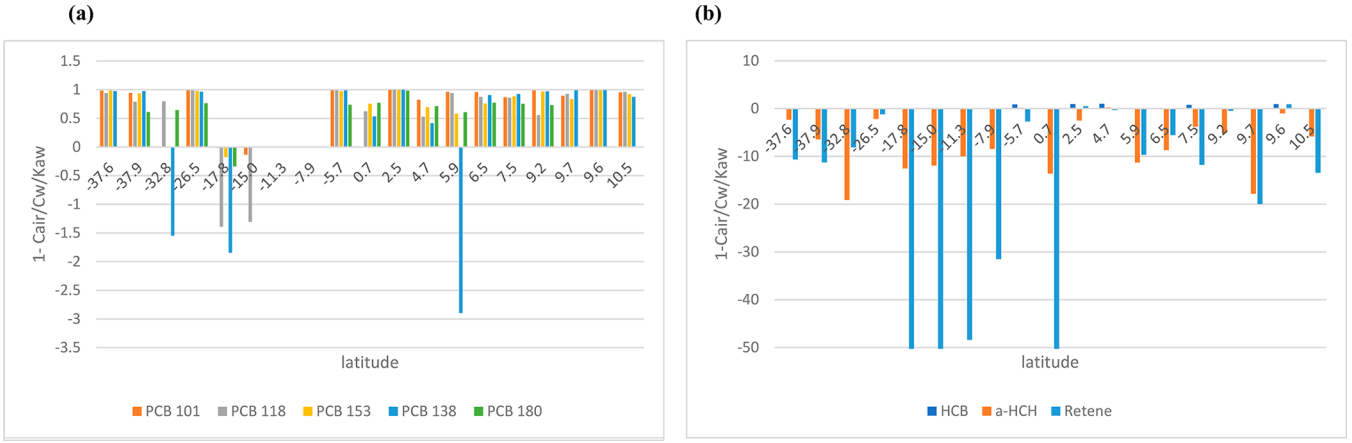

Figure 4. Air−water exchange fugacity calculations for (a) PCB congeners 101, 118, 153, 138, and 180 and (b) *a*-HCH, HCB, and retene as a function of degree latitude. A value greater than 0 indicates net volatilization; a value smaller than 0 indicates net deposition. As needed, 1/2 MDL was substituted for PCB congeners in the air for the calculations and for *a*-HCH in the water for the calculations.

pg/L, and fluoranthene at 12 (4) pg/L (see SI). These southern Atlantic Ocean equatorial samples are unlikely to be affected to sampling contamination and probably reflect low PAH concentrations resulting from long-range transport from across Africa.

Others have reported widely diverging concentrations of dissolved PAHs: in the range of 100s of pg/L for individual PAHs in the North Pacific and Arctic Ocean.[20] Even greater concentrations have been reported for the Russian Arctic,[50] the western Pacific, and Southern Ocean.[51] Lowest concentrations were reported by Ma et al.[43] for the western Pacific and Arctic Ocean on the order of 10s−100s pg/L for individual PAHs, similar to results by Lohmann et al.[44] across the tropical Atlantic Ocean.

Dissolved POPs Gradients Across the Western Tropical Atlantic Ocean. Concentrations of dissolved PCBs/OCPs and PBDEs can be grouped into four different regions: (i) between 20 and 40°S, with the routine detection of higher molecular weight PCBs, *α*-HCH, and *β*-HCH and BDE 47. Most likely, the pollutants originated from the Rio de la Plata plume, which mixes across the shelf during the summer, while during the winter months, it hugs northwards along the coast;[37] (ii) between 20°S and the equator, most POPs were <MDL. This region is influenced by the Brazil Current, moving water masses originating from off Africa, as part of the South Equatorial Current, southwards along the continent. These water masses only possessed trace amount of POPs, as can be explained by a long residence time enabling biogeochemical processes to deplete compounds either via photolysis, microbial degradation, or settling as part of the biological pump;[13,52] (iii) there was a spike in contaminant concentrations at around 2−5°N, which could represent the northern part of the South Equatorial Current, where some North Atlantic water is already entrained from the North Equatorial Counter Current;[53] (iv) the region between 6 and 11°N, where there was a fairly stable signature of PCBs and HCBs but a lack of PBDEs. Samples taken between 9.7 and 11°N represented water masses that were affected by the Amazon and Orinoco river discharges (given the decrease in salinity). There were no significant correlations with water temperature, salinity, or fluorescence for aqueous HOC concentrations across the entire sampling region.

Air−Water Exchange. For a total of 19 matching air and water samples, fugacity gradients across the air−water interface were calculated, such that values >0 indicated net volatilization, 0 indicated equilibrium, and <0 indicated net deposition. For PCB congeners 101, 118, 138, 153, and 180, there was, across most stations, a strong gradient favoring net volatilization from the surface ocean to the overlying atmosphere (Figure 4a). In other words, PCB fugacities in the dissolved phase were greater than in the atmosphere. The exception were a couple of samples at around 15−20°S in which a decrease in dissolved concentrations coupled with the detection of those PCB congeners in the atmosphere reversed the measured gradient toward net deposition. The calculated gradients were based on the substitution of non-detects with 1/2 MDL in the gas-phase (note that substitution with the full MDL changed the gradient in only 3 out of 91 cases). A lack of detection of PCBs in water and air at around 8−11°S prevented us from deducing the direction of air−water exchange. Lastly, air−water exchange gradients could not be established for low- molecular weight PCBs due to a lack of their detection in the dissolved phase.

The importance of volatilization for PCBs was predicted by a coupled global atmosphere−ocean model; it suggested that the tropical and southern Atlantic Ocean was one of the regions where volatilization was particularly important releasing 6−17% of the total PCB budget in the upper 1000 m of the ocean annually.[33] By contrast, modeled atmospheric deposition was the dominant input pathway for PCBs in the North Atlantic Ocean. Mass flow of PCBs with ocean circulation constitutes an important source for the tropical and southern Atlantic (17−61% of inputs).[33]

A very different picture emerged for *a*-HCH for which there was a gradient favoring net deposition from the gas-phase across all sites (Figure 4b). This was driven by the constant detection of *a*-HCH in the gas phase but a lack of its detection in the dissolved phase. One exception at 5°N was caused by the detection of *a*-HCH in the dissolved phase, coupled with a decreased gas-phase concentrations. The calculated gradients were based on the substitution of 1/2 MDL in the dissolved phase (note that substitution of MDL did not affect the gradient in all cases but the sample pair at 3°N).

For HCB, we were able to deduce air-water exchange gradients only at few sites, but at those, we typically derived net volatilization (Figure 4b). This result is not surprising,

https://dx.doi.org/10.1021/acs.est.0c04611
Environ. Sci. Technol. XXXX, XXX, XXX−XXX

given that HCB is assumed to be closer to equilibrium distributions in the environment relative to other POPs.[54] Strong spatial gradients have been reported for the air−water exchange of PCBs and OCPs: generally net deposition for the (biologically productive) North Atlantic,[15,38,45] but equilibrium or net evaporation for the tropical and South Atlantic Ocean,[23,55] in-line with results reported here.

Lastly, for PAHs, a few general trends can be reported: while retene routinely underwent net deposition, air−water exchange gradients of other PAHs varied strongly by region. Between 18°S and 1°N, all PAHs typically displayed net deposition, but gradients flipped beyond that region.

Across our study region, air and water concentrations were not significantly (positively) correlated with either air or water temperature, salinity, or wind speed, indicating that other factors dominated. We hence expect that the direction of air−water exchange fluxes for the target compounds will not vary much throughout the year, given that the tropical region investigated here is not prone to major temperature changes throughout the year. Overall, we can summarize that riverine plumes (Rio de la Plata, Orinoco/Amazon) served to release and distribute POPs in the water, causing volatilization of most POPs away from the coasts, with the exception of regions where atmospheric pulses temporarily dominate, resulting in net gas-phase deposition. Yet the major South Equatorial surface current, by the time it reached the South American continent, contained little to no POPs.

Comparison of Measured Concentrations Relative to Global Model Results. We compared our measured PCB concentrations in the surface ocean to the predictions from the Wagner et al. (2019) global ocean model (Figure 5): as best as we know, it is the only existing ocean model for hydrophobic POPs. The spatial patterns in PCB concentrations between measurements and model results were in agreement with a maximum in the South Atlantic near Brazil between 20 and 30°S, lowest concentrations around the equator, and another increase at around 5−10°N. In terms of actual concentrations, measured concentrations exceeded predictions by up to 4 orders of magnitude for CB-28. These results were consistent with those reported by Wagner et al. (2019), which suggested that the Breivik et al. inventory was missing contemporary PCB sources in the southern hemisphere. Prior work suggests that substantial releases to the South Atlantic originate from recycling activities in West Africa.[15,56] Aquatic transport of PCBs, such as from West Africa with the SEC, will lead to preferential losses of heavier congeners due to losses with photolysis, microbial degradation, or settling. The more pronounced underestimation of concentrations of PCB-28 and PCB-101 may thus be evidence of nonlocal sources to the West Atlantic.

Implications. Surprisingly, there were no major gradients in atmospheric concentrations between SH and NH; this might be an indication that as direct emissions (mostly in the NH) have ceased, both hemispheres are slowly approaching the same concentrations. At the same time, it is equally possible that these results are only reflective of the particular region we investigated (possibly reflecting additional POPs emissions from Western Africa) and not (yet) indicative of larger global atmospheric trends.

Results from the tropical West Atlantic highlighted and confirmed the importance of water masses for the detection of POPs. The cruise displayed sharp gradients of most targeted POPs in the southern Atlantic Ocean: their routine detection

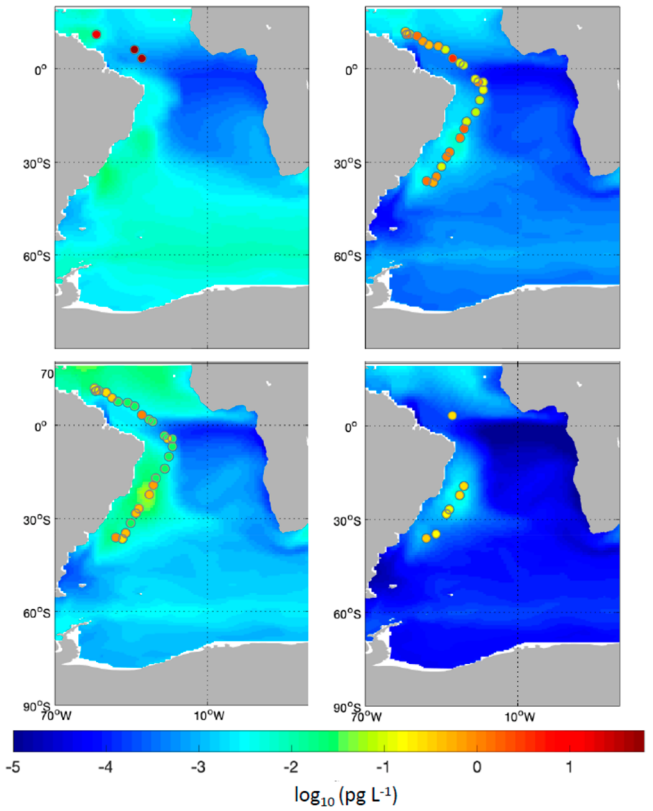

Figure 5. Comparison of measured versus modeled PCB concentrations for the Atlantic Ocean (from top left clock-wise PCB 28, 101, 153, and 180).

in water masses influenced by the Rio de la Plata, but a complete lack of detection in the South Equatorial/Brazil Current. This resulted also in a reversal of air−water exchange gradients of PCBs, from a general volatilization in regions impacted by river plumes to net deposition in the South Equatorial/Brazil Current. A sharp increase of POPs just north of the equator is probably an indication of the intense cycling of compounds affected by the ITCZ and its frequent rains, causing elevated concentrations in water, which in turn cause their revolatilization. Overall, then, we observed strong heterogeneity in ocean concentrations, which mirrored trends predicted by a global coupled atmosphere−ocean model for PCB concentrations; see Figure 3. Yet the model underpredicted aqueous concentrations, possibly due to missing land-based sources.

■ ASSOCIATED CONTENT

Supporting Information

The Supporting Information is available free of charge at https://pubs.acs.org/doi/10.1021/acs.est.0c04611.

Physicochemical constants, instrumental analysis and QC, sampling setup and sample details, air and water concentrations (PDF)

■ AUTHOR INFORMATION

Corresponding Author

Rainer Lohmann − *Graduate School of Oceanography, University of Rhode Island, 02882 Rhode, Island, United States;* orcid.org/0000-0001-8796-3229; Phone: (401) 874-6612; Email: rlohmann@uri.edu; Fax: (401) 874-6811

https://dx.doi.org/10.1021/acs.est.0c04611
Environ. Sci. Technol. XXXX, XXX, XXX−XXX

Authors

Erin Markham − *Graduate School of Oceanography, University of Rhode Island, 02882 Rhode, Island, United States*

Jana Klanova − *Research Centre for Toxic Compounds in the Environment (RECETOX), Faculty of Science, Masaryk University, 625 00 Brno, Czech Republic*

Petr Kukucka − *Research Centre for Toxic Compounds in the Environment (RECETOX), Faculty of Science, Masaryk University, 625 00 Brno, Czech Republic*

Petra Pribylova − *Research Centre for Toxic Compounds in the Environment (RECETOX), Faculty of Science, Masaryk University, 625 00 Brno, Czech Republic*

Xiangyi Gong − *Graduate School of Oceanography, University of Rhode Island, 02882 Rhode, Island, United States; College of Resources and Environmental Engineering, Wuhan University of Science and Technology, Wuhan 430081, China*

Robert Pockalny − *Graduate School of Oceanography, University of Rhode Island, 02882 Rhode, Island, United States*

Tatyana Yanishevsky − *Graduate School of Oceanography, University of Rhode Island, 02882 Rhode, Island, United States*

Charlotte C. Wagner − *Harvard John A. Paulson School of Engineering and Applied Science, Harvard University, Cambridge, Massachusetts 02138, United States*

Elsie M. Sunderland − *Harvard John A. Paulson School of Engineering and Applied Science, Harvard University, Cambridge, Massachusetts 02138, United States;* orcid.org/0000-0003-0386-9548

Complete contact information is available at: https://pubs.acs.org/10.1021/acs.est.0c04611

Notes

The authors declare no competing financial interest.

■ ACKNOWLEDGMENTS

R Lohmann expresses his gratitude for K.C. Jones for his mentorship during his PhD and beyond. The cruise was supported by the National Science Foundation (grant #OCE-1154320 to E. Kujawinski and K. Longnecker, WHOI). We thank the captain and crew of the *R/V* Knorr for their assistance with sampling, and R Pockalny (URI) for help with Figure [1]. This research received financial support from the CETOCOEN EXCELLENCE Teaming 2 project supported by Horizon2020 (857560) and the Czech Ministry of Education, Youth and Sports (02.1.01/0.0/0.0/18_046/0015975), and the RECETOX research infrastructure (the Czech Ministry of Education, Youth and Sports: LM2018121).

■ REFERENCES

(1) Wania, F.; Mackay, D. Tracking the Distribution of Persistent Organic Pollutants. *Environ. Sci. Technol.* **1996**, *30* (9), 390A−396A.

(2) Bidleman, T. F.; Olney, C. E. Chlorinated Hydrocarbons in the Sargasso Sea Atmosphere and Surface Water. *Science (Washington, DC, U. S.)* **1974**, *183* (4124), 516−518.

(3) Meijer, S. N.; Ockenden, W. A. Global Distribution and Budget of PCBs and HCB in Background Surface Soils: Implications for Sources and Environmental Processes. *Environ. Sci. Technol.* **2003**, *37*, 667−672.

(4) Kalantzi, O. I.; Alcock, R. E. The Global Distribution of PCBs and Organochlorine Pesticides in Butter. *Environ. Sci. Technol.* **2001**, *35* (6), 1013−1018.

(5) Hargrave, B. T.; Vass, W. P.; Erickson, P. E.; Fowler, B. R. Atmospheric Transport of Organochlorines to the Arctic Ocean. *Tellus, Ser. B* **1988**, *40B* (5), 480−493.

(6) Risebrough, R. W.; Walker, W., II; Schmidt, T. T.; De Lappe, B. W.; Connors, C. W. Transfer of Chlorinated Biphenyls to Antarctica. *Nature* **1976**, *264* (5588), 738−739.

(7) Jonsson, A.; Gustafsson, Ö.; Axelman, J.; Sundberg, H. Global Accounting of PCBs in the Continental Shelf Sediments. *Environ. Sci. Technol.* **2003**, *37*, 245−255.

(8) Laflamme, R. E.; Hites, R. A. The Global Distribution of Polycyclic Aromatic Hydrocarbons in Recent Sediments. *Geochim. Cosmochim. Acta* **1978**, *42* (3), 289−303.

(9) Kramer, W.; Ballschmiter, K. Global Baseline Pollution Studies XII. Content and Pattern of Polychloro-Cyclohexanes (HCH) and -Bi-Phenyls (PCB), and Content of Hexachlorobenzene in the Water Column of the Atlantic Ocean. *Fresenius' Z. Anal. Chem.* **1988**, *330*, 524−526.

(10) Iwata, H.; Tanabe, S.; Sakal, N.; Tatsukawa, R. Distribution of Persistent Organochlorines in the Oceanic Air and Surface Seawater and the Role of Ocean on Their Global Transport and Fate. *Environ. Sci. Technol.* **1993**, *27* (6), 1080−1098.

(11) Lohmann, R.; Jaward, F. M.; Durham, L.; Barber, J. L.; Ockenden, W.; Jones, K. C.; Bruhn, R.; Lakaschus, S.; Dachs, J.; Booij, K. Potential Contamination of Shipboard Air Samples by Diffusive Emissions of PCBs and Other Organic Pollutants: Implications and Solutions. *Environ. Sci. Technol.* **2004**, *38* (14), 3965.

(12) González-Gaya, B.; Dachs, J.; Roscales, J. L.; Caballero, G.; Jiménez, B. Perfluoroalkylated Substances in the Global Tropical and Subtropical Surface Oceans. *Environ. Sci. Technol.* **2014**, *48* (22), 13076−13084.

(13) Morales, L.; Dachs, J.; Fernández-Pinos, M. C.; Berrojalbiz, N.; Mompean, C.; González-Gaya, B.; Jiménez, B.; Bode, A.; Ábalos, M.; Abad, E. Oceanic Sink and Biogeochemical Controls on the Accumulation of Polychlorinated Dibenzo-p-Dioxins, Dibenzofurans, and Biphenyls in Plankton. *Environ. Sci. Technol.* **2015**, *49* (23), 13853−13861.

(14) Castro-Jiménez, J.; González-Gaya, B.; Pizarro, M.; Casal, P.; Pizarro-Álvarez, C.; Dachs, J. Organophosphate Ester Flame Retardants and Plasticizers in the Global Oceanic Atmosphere. *Environ. Sci. Technol.* **2016**, *50* (23), 12831−12839.

(15) Gioia, R.; Lohmann, R.; Dachs, J.; Temme, C.; Lakaschus, S.; Schulz-Bull, D.; Hand, I.; Jones, K. C. Polychlorinated Biphenyls in Air and Water of the North Atlantic and Arctic Ocean. *J. Geophys. Res.* **2008**, *113* (19), 9750 DOI: 10.1029/2007JD009750.

(16) Xie, Z.; Koch, B. P.; Möller, A.; Sturm, R.; Ebinghaus, R. Transport and Fate of Hexachlorocyclohexanes in the Oceanic Air and Surface Seawater. *Biogeosciences* **2011**, *8* (9), 2621−2633.

(17) Li, J.; Xie, Z.; Mi, W.; Lai, S.; Tian, C.; Emeis, K. C.; Ebinghaus, R. Organophosphate Esters in Air, Snow, and Seawater in the North Atlantic and the Arctic. *Environ. Sci. Technol.* **2017**, *51* (12), 6887−6896.

(18) Jaward, F. M.; Barber, J. L.; Booij, K.; Dachs, J.; Lohmann, R.; Jones, K. C. Evidence for Dynamic Air-Water Coupling and Cycling of Persistent Organic Pollutants over the Open Atlantic Ocean. *Environ. Sci. Technol.* **2004**, *38* (9), 2617.

(19) Cai, M.; Liu, M.; Hong, Q.; Lin, J.; Huang, P.; Hong, J.; Wang, J.; Zhao, W.; Chen, M.; Cai, M.; Ye, J. Fate of Polycyclic Aromatic Hydrocarbons in Seawater from the Western Pacific to the Southern Ocean (17.5°N to 69.2°S) and Their Inventories on the Antarctic Shelf. *Environ. Sci. Technol.* **2016**, *50* (17), 9161−9168.

(20) Ke, H.; Chen, M.; Liu, M.; Chen, M.; Duan, M.; Huang, P.; Hong, J.; Lin, Y.; Cheng, S.; Wang, X.; Huang, M.; Cai, M. Fate of Polycyclic Aromatic Hydrocarbons from the North Pacific to the Arctic: Field Measurements and Fugacity Model Simulation. *Chemosphere* **2017**, *184*, 916−923.

(21) Bigot, M.; Muir, D. C. G.; Hawker, D. W.; Cropp, R.; Dachs, J.; Teixeira, C. F.; Bengtson Nash, S. Air-Seawater Exchange of Organochlorine Pesticides in the Southern Ocean between Australia and Antarctica. *Environ. Sci. Technol.* **2016**, *50* (15), 8001−8009.

(22) Xie, Z.; Möller, A.; Ahrens, L.; Sturm, R.; Ebinghaus, R. Brominated Flame Retardants in Seawater and Atmosphere of the

Atlantic and the Southern Ocean. *Environ. Sci. Technol.* **2011**, *45* (5), 1820−1826.
(23) Lohmann, R.; Klanova, J.; Kukucka, P.; Yonis, S.; Bollinger, K. PCBs and OCPs on a East-to-West Transect: The Importance of Major Currents and Net Volatilization for PCBs in the Atlantic Ocean. *Environ. Sci. Technol.* **2012**, *46* (19), 10471.
(24) Lohmann, R.; Belkin, I. M. Organic Pollutants and Ocean Fronts across the Atlantic Ocean: A Review. *Prog. Oceanogr.* **2014**, *128*, 172.
(25) Antweiler, R. C.; Taylor, H. E. Evaluation of Statistical Treatments of Left-Censored Environmental Data Using Coincident Uncensored Data Sets: I. Summary Statistics. *Environ. Sci. Technol.* **2008**, *42* (10), 3732−3738.
(26) Beyer, A.; Wania, F.; Gouin, T.; Mackay, D.; Matthies, M. Selecting Internally Consistent Physicochemical Properties of Organic Compounds. *Environ. Toxicol. Chem.* **2002**, *21* (5), 941−953.
(27) Schenker, U.; MacLeod, M.; Scheringer, M.; Hungerbühler, K. Improving Data Quality for Environmental Fate Models: A Least-Squares Adjustment Procedure for Harmonizing Physicochemical Properties of Organic Compounds. *Environ. Sci. Technol.* **2005**, *39* (21), 8434−8441.
(28) Jonker, M. T. O.; Muijs, B. Using Solid Phase Micro Extraction to Determine Salting-out (Setschenow) Constants for Hydrophobic Organic Chemicals. *Chemosphere* **2010**, *80* (3), 223−227.
(29) Siegel, D. A.; Maritorena, S.; Nelson, N. B.; Hansell, D. A.; Lorenzi-Kayser, M. Global Distribution and Dynamics of Colored Dissolved and Detrital Organic Materials. *J. Geophys. Res. C Ocean.* **2002**, *107* (C12), 21-1−1.
(30) Burkhard, L. P. Estimating Dissolved Organic Carbon Partition Coefficients for Nonionic Organic Chemicals. *Environ. Sci. Technol.* **2000**, *34* (22), 4663−4668.
(31) Rolph, G.; Stein, A.; Stunder, B. Real-Time Environmental Applications and Display SYstem: READY. *Environ. Model. Softw.* **2017**, *95*, 210−228.
(32) Stein, A. F.; Draxler, R. R.; Rolph, G. D.; Stunder, B. J. B.; Cohen, M. D.; Ngan, F. Noaa's Hysplit Atmospheric Transport and Dispersion Modeling System. *Bull. Am. Meteorol. Soc.* **2015**, *96* (12), 2059−2077.
(33) Wagner, C. C.; Amos, H. M.; Thackray, C. P.; Zhang, Y.; Lundgren, E. W.; Forget, G.; Friedman, C. L.; Selin, N. E.; Lohmann, R.; Sunderland, E. M. A Global 3-D Ocean Model for PCBs: Benchmark Compounds for Understanding the Impacts of Global Change on Neutral Persistent Organic Pollutants. *Global Biogeochem. Cycles* **2019**, *33* (3), 469−481.
(34) Breivik, K.; Sweetman, A.; Pacyna, J. M.; Jones, K. C. Towards a Global Historical Emission Inventory for Selected PCB Congeners - A Mass Balance Approach. 3. An Update. *Sci. Total Environ.* **2007**, *377* (2−3), 296−307.
(35) Breivik, K.; Sweetman, A.; Pacyna, J. M.; Jones, K. C. Towards a Global Historical Emission Inventory for Selected PCB Congeners - A Mass Balance Approach: 2. Emissions. *Sci. Total Environ.* **2002**, *290* (1−3), 199−224.
(36) Friedman, C. L.; Selin, N. E. PCBs in the Arctic Atmosphere: Determining Important Driving Forces Using a Global Atmospheric Transport Model. *Atmos. Chem. Phys.* **2016**, *16* (5), 3433−3448.
(37) Burrage, D.; Wesson, J.; Martinez, C.; Pérez, T.; Möller, O.; Piola, A. Patos Lagoon Outflow within the Río de La Plata Plume Using an Airborne Salinity Mapper: Observing an Embedded Plume. *Cont. Shelf Res.* **2008**, *28* (13), 1625−1638.
(38) Zhang, L.; Thibodeaux, L.; Jones, L.; Lohmann, R. Simulation of Observed PCBs and Pesticides in the Water Column during the North Atlantic Bloom Experiment. *Environ. Sci. Technol.* **2015**, *49* (23), 13760.
(39) Pegoraro, C. N.; Harner, T.; Su, K.; Chiappero, M. S. Assessing Levels of POPs in Air over the South Atlantic Ocean off the Coast of South America. *Sci. Total Environ.* **2016**, *571*, 172−177.
(40) Chao, H. R.; Lin, D. Y.; Chen, K. Y.; Gou, Y. Y.; Chiou, T. H.; Lee, W. J.; Chen, S. J.; Wang, L. C. Atmospheric Concentrations of Persistent Organic Pollutants over the Pacific Ocean near Southern Taiwan and the Northern Philippines. *Sci. Total Environ.* **2014**, *491*−*492* (219), 51−59.
(41) Lohmann, R.; Klanova, J.; Kukucka, P.; Yonis, S.; Bollinger, K. Concentrations, Fluxes, and Residence Time of PBDEs across the Tropical Atlantic Ocean. *Environ. Sci. Technol.* **2013**, *47* (24), 13967.
(42) Ramdahl, T. Retene - a Molecular Marker of Wood Combustion in Ambient Air. *Nature* **1983**, *306*, 580−582.
(43) Ma, Y.; Xie, Z.; Yang, H.; Möller, A.; Halsall, C.; Cai, M.; Sturm, R.; Ebinghaus, R. Deposition of Polycyclic Aromatic Hydrocarbons in the North Pacific and the Arctic. *J. Geophys. Res. Atmos.* **2013**, *118* (11), 5822−5829.
(44) Lohmann, R.; Klanova, J.; Pribylova, P.; Liskova, H.; Yonis, S.; Bollinger, K. PAHs on a West-to-East Transect across the Tropical Atlantic Ocean. *Environ. Sci. Technol.* **2013**, *47* (6), 2570.
(45) González-Gaya, B.; Fernández-Pinos, M. C.; Morales, L.; Méjanelle, L.; Abad, E.; Piña, B.; Duarte, C. M.; Jiménez, B.; Dachs, J. High Atmosphere-Ocean Exchange of Semivolatile Aromatic Hydrocarbons. *Nat. Geosci.* **2016**, *9* (6), 438−442.
(46) Soerensen, A. L.; Mason, R. P.; Balcom, P. H.; Jacob, D. J.; Zhang, Y.; Kuss, J.; Sunderland, E. M. Elemental Mercury Concentrations and Fluxes in the Tropical Atmosphere and Ocean. *Environ. Sci. Technol.* **2014**, *48*, 11312−11319.
(47) Lammel, G.; Spitzy, A.; Audy, O.; Beckmann, S.; Codling, G. P.; Kretzschmann, L.; Kukučka, P.; Stemmler, I. Organochlorine Pesticides and Polychlorinated Biphenyls along an East-to-West Gradient in Subtropical North Atlantic Surface Water. *Environ. Sci. Pollut. Res.* **2017**, *24* (12), 11045−11052.
(48) Abbasi, G.; Buser, A. M.; Soehl, A.; Murray, M. W.; Diamond, M. L. Stocks and Flows of PBDEs in Products from Use to Waste in the U.S. and Canada from 1970 to 2020. *Environ. Sci. Technol.* **2015**, *49* (3), 1521−1528.
(49) Wu, Z.; Lin, T.; Guo, T.; Li, Y.; Li, Z.; Guo, Z. Occurrence, Air-Sea Exchange, and Gas-Particle Partitioning of Atmospheric Polybrominated Diphenyl Ethers from East Asia to the Northwest Pacific Ocean. *Chemosphere* **2020**, *240*, 124933.
(50) Ji, X.; Abakumov, E.; Xie, X. Atmosphere-Ocean Exchange of Heavy Metals and Polycyclic Aromatic Hydrocarbons in the Russian Arctic Ocean. *Atmos. Chem. Phys.* **2019**, *19* (22), 13789−13807.
(51) Cai, M.; Liu, M.; Hong, Q.; Lin, J.; Huang, P.; Hong, J.; Wang, J.; Zhao, W.; Chen, M.; Cai, M.; Ye, J. Fate of Polycyclic Aromatic Hydrocarbons in Seawater from the Western Pacific to the Southern Ocean (17.5°N to 69.2°S) and Their Inventories on the Antarctic Shelf. *Environ. Sci. Technol.* **2016**, *50* (17), 9161−9168.
(52) Galbán-Malagón, C. J.; Berrojalbiz, N.; Gioia, R.; Dachs, J. The "Degradative" and "Biological" Pumps Controls on the Atmospheric Deposition and Sequestration of Hexachlorocyclohexanes and Hexachlorobenzene in the North Atlantic and Arctic Oceans. *Environ. Sci. Technol.* **2013**, *47* (13), 7195−7203.
(53) University of Miami Rosenstiel School of Marine and Atmoshperic Science (RSMAS). Ocean Surface Currents https://oceancurrents.rsmas.miami.edu/index.html (accessed Jun 29, 2020).
(54) Barber, J. L.; Sweetman, A. J.; van Wijk, D.; Jones, K. C. Hexachlorobenzene in the Global Environment: Emissions, Levels, Distribution, Trends and Processes. *Sci. Total Environ.* **2005**, *349*, 1−44.
(55) Gioia, R.; Nizzetto, L.; Lohmann, R.; Dachs, J.; Temme, C.; Jones, K. C. Polychlorinated Biphenyls (PCBs) in Air and Seawater of the Atlantic Ocean: Sources, Trends and Processes. *Environ. Sci. Technol.* **2008**, *42* (5), 1416.
(56) Gioia, R.; Eckhardt, S.; Breivik, K.; Jaward, F. M.; Prieto, A.; Nizzetto, L.; Jones, K. C. Evidence for Major Emissions of PCBs in the West African Region. *Environ. Sci. Technol.* **2011**, *45* (4), 1349−1355.
(57) Wessel, P.; Smith, W. H. F.; Scharroo, R.; Luis, J.; Wobbe, F. Generic Mapping Tools: Improved Version Released. *EOS Trans. AGU* **2013**, *94* (45), 409−410.
(58) Ocean Biology Processing Group. MODIS Aqua Level 3 Global Monthly Mapped 4 km Chlorophyll a v2014.0. Ver. 2014.0. PO.DAAC, CA, USA (**2015**).

https://dx.doi.org/10.1021/acs.est.0c04611
Environ. Sci. Technol. XXXX, XXX, XXX−XXX